Nat. Hazards Earth Syst. Sci. Discuss., 3, 5015–5044, 2015
www.nat-hazards-earth-syst-sci-discuss.net/3/5015/2015/
doi:10.5194/nhessd-3-5015-2015

Natural Hazards and Earth System Sciences Discussions
Open Access

The quantitative estimation of the vulnerability of brick and concrete building impacted by debris flow

J. Zhang[1,2], Z. X. Guo[2], D. Wang[2,3], and H. Qian[2,4]

[1]School of Energy and Power Engineering, Xihua University, Chengdu, 610039, China
[2]State Key Laboratory of Hydraulics and Mountain River Engineering, Sichuan University, Chengdu, 610065, China
[3]Highway Planning Survey & Design Institute, Sichuan Communications Department, Chengdu, 610041, China
[4]Chengdu Municipal Engineering Design and Research Institute, Chengdu, 610015, China

Received: 18 July 2015 – Accepted: 27 July 2015 – Published: 26 August 2015

Correspondence to: J. Zhang (phyllis_zj@yeah.net)

Published by Copernicus Publications on behalf of the European Geosciences Union.

Abstract

There is little historic data about the vulnerability of the damage elements in debris flow disaster in China. Therefore, it is difficult to estimate the vulnerability of debris flow quantitatively. This paper was devoted to the research of the vulnerability of brick and concrete building impacted by debris flow which widely existed in affected area. Under two assumptions, several prototype walls of brick and concrete were constructed to simulate the damaged structures in debris flow while the iron spheres were taken as the substitute of debris flow. The failure criterion of brick and concrete building was proposed with referring to the structure standards (brick and concrete) and the damage pattern in debris flow. The quantitatively estimation of vulnerability of brick and concrete building was finally established based on Fuzzy mathematics and the proposed failure criterion. The results show that the maximum impact bending moment is the best fit to be the disaster-causing factor in vulnerability curve and formula. The experiments in this paper is the preliminary research on the vulnerability of the element impacted by debris flow. The method and conclusion will be useful for the quantitative estimation of the vulnerability in debris flow and also can be referred in other types of the vulnerable elements research.

1 Introduction

After Wenchuan Earthquake, several catastrophic earthquake events in high magnitude (> 6.5) occurred in China recently. For example, Yushu earthquake in Qinghan on 14 April 2010; Lushan earthquake in Yaan, Sichuan on 20 April 2013; Ludian earthquake in Zhaotong, Yunnan on 3 August 2014 (Earthquake in China). Huge volume of the deposit induced by earthquake contribute to new debris flows in more frequency and lager magnitude leading much losses both in life and economic (Tang et al., 2011b). As an efficient method to natural hazards, risk estimation is popular in debris flow work. Quantitative vulnerability estimation is a necessary element of

NHESSD
3, 5015–5044, 2015

risk estimation. During decades, however, the vulnerability research of debris flow had a slow development for several reasons: first, it was widely accepted that the behavior of debris flow was quite complicated and had not be clearly revealed yet (Rickenmann, 1999; Cui, 2009); second, there are many kinds of vulnerability elements attacked by debris flow and the indicator system involves many influence factors not only in natural vulnerability but also in social vulnerability (for example, economic, environment and human) (Liu et al., 2012); third, historic data is much of use in estimating vulnerability with statistic method and in improving the accuracy. Unfortunately, most of the database and reports are about characteristic of debris flow not element vulnerability (Tang et al., 2011a; Zhang et al., 2013); four, the lack of vulnerability results is also relevant to the little attention from both engineers and scientists in past years. Unlike earthquake and cyclone, structural measure is capable to decrease the damage of debris flow (Douglas, 2007).

There are mainly four evaluation methods for debris flow vulnerability: multi-index assessment, element value accounting, empirical vulnerability curve and model experiment. Among these, the first two methods were widely applied in China for region vulnerability estimation of debris flow based on the category of affected elements and the market value of the elements. They are, therefore, suitable for the regions of large area and high density elements, but fail to connect with the debris flow intensity (Liu et al., 2001; Tang et al., 2005; Tie, 2009). Empirical vulnerability curve was raised by European researchers. The curves were fitted with the empirical data of investigated house which included the deposit height and the vulnerability of the element (Papathoma et al., 2011). At beginning, the vulnerability was qualitative, but after soon people realized that only quantitative data could lead effective evaluation (Bell et al., 2004; Romang, 2004; Michael et al., 2003). The first curve was provided by Fuchs (2007) according to the debris flow event in the Austrian Alps. Then, Totschnig (2011) applied Modified Frechet no.2 distribution instead of polynomial to fit the numerous data from three databases. Kinematic velocity and impact pressure could also be the disaster intensity factors of vulnerability if the numerical simulation of debris flow could be conducted (Luna, 2011).

So far, vulnerability curves of debris flow were mostly established based on the historic data or investigation. However, few useful data could be applied for vulnerability curve in China since the main attention of engineering and government paid on the disaster itself and resettlement of disaster-affected elements. In this case, experiments can be an alternative method. The primary damage of building occurred during the deposit process of debris flow. In order to provide the reference load for the design of check dam in material and structure, the impact force researches before, however, focused on the critical value of element destruction and the characteristic of debris flow head (Hübl, 2005; Wang, 2001; Chen et al., 2010) rather than the response of suffered elements. Thus, it is hard to draw vulnerability curves from the debris flow impact force researches before. Borrowing the evaluation model of earthquake did not work well probably because the destruction mechanisms of building induced by these two disasters were different (HAZUS, 2006; Haugen et al., 2008). Brick and concrete building is the typical civil architecture in southwestern mountain area of China. Generally, the destruction of load-bearing wall directly lead to the collapse of house. Zhang (2005) have studied the ultimate load-bearing capacity of brick and concrete wall in 1 : 2 scale attacked by a substitute of debris flow. There are two problems if the vulnerability curve is going to be drawn from this kind of experiments:

1. Vulnerability curve contains various damage degrees of the building while, in her research, only the destruction status was concerned.

2. Though the function between load and geometry of wall still stays blank, it should be a complicate expression. Thus, vulnerability evaluation cannot be applied in prototype since the similarity law between load and geometry is unknown.

NHESSD
3, 5015–5044, 2015

2 Experiment description

2.1 Assumption

The experiments here were conducted on the purpose of the vulnerability curve of brick and concrete building which was prototype and had only one story. Since the collapse of building was mainly caused by the destruction of load-bearing wall, the object attacked in experiment was the load-bearing wall but not the whole building. Producing debris flow with a specific momentum is difficult, iron spheres can be a good choice for the simulation of debris flow impact (Zhang, 2005). There are two assumptions in the experiments below:

1. Debris flow is consisted of slurry and particles. Slurry produces uniform load on the wall while particles, of which the size vary in great range, produce concentrated load. Both the impact value and site of the particles on the wall are random and the rock fall researches (Mavrouli et al., 2010) could provide good reference. Here, only uniform load induced by slurry was considered in this study.

2. The actual impact force is $F \cdot \cos\alpha$, in which α is the intersection angle of the impact force and the wall surface. In this study, debris flow is assumed to attack the wall vertically ($\alpha = 90^\circ$).

2.2 Experiment set up

At the beginning of the experiments, the iron sphere, which was jointed to the top of the supporting frame with a chain, was dragged by the dynamic system up to a certain height of the operation platform. When the system power was off, the sphere would fall in a circle under gravity force and then hit the middle of the iron board in front of the wall. The iron board could spread the concentrated load onto the area of the wall that the board covered. A rubber cushion was set between the board and the wall to delay

NHESSD
3, 5015–5044, 2015

the attack time and homogenize the force onto the wall. The experiment set up was shown in Fig. 1.

As shown in Fig. 1, the operation platform had three height to choose: 3, 4, and 5 m. The debris flow in various magnitude was simulated by releasing different sphere from different height. In the experiments, the length of chain and the height of iron board were both adjustable.

According to Brick and Concrete Structural Design Manual of China, the standard load-bearing wall was 240 mm thick, 3.0 m high and 3.0 m wide. The net height of wall was 2.7 m and the foundation that was 0.3 m deep was made with reinforced concrete (see Fig. 2). Try to smooth the surface of wall to make sure the well contact between the wall and the board.

2.3 Apparatus

An impact force gauge system including a sensor and a peak force instrument was applied to obtain the force suffered by the load-bearing wall during the impact process. The sensor fixed onto the back of the wall firstly changed the weight signal of force to electronic signal; then the electronic signal became digital display on the instrument; At last the impact force graph during the whole process could be read and recorded by the computer. The sample frequency here was 100 Hz. The maximum dynamic displacement and static displacement were measured by self-made displacement gauge. The inclination of the wall i equaled to the ratio of the maximum dynamic displacement ΔL_{dd} and the height of the wall H. The cracks with different width could be identified by a crack comparing ruler which can distinguish the cracks wider than 0.1 mm. The camera recorded the experiments process.

2.4 Conditions

According to the historic debris flow events in China, the parameters of debris flow vary in a wide range (Generally, the density ρ is 1.2–2.3 g cm^{-3}; the velocity v is 3–

NHESSD
3, 5015–5044, 2015

10 m s^{-1}; the flow depth h is 0–10 m). It is unreasonable to employ any parameter alone to represent the disaster intense of debris flow, while momentum can be good choice. The momentum range in these experiments can be calculated by using $mv = \rho bhv^2$. In view of the size of lab site and the sufferance of the object, the weights of the iron sphere are 47 and 86 kg determined by back stepping with the platform height (ρ is 2.2 g cm^{-3}). The board in front of the wall represents the depth of debris flow that is 1, 1.5 and 2 m. Therefore, there are totally nine experiments and they are numbered as A1, A2, A2, B1, B2, B3, C1, C2, C3. The experiments condition are explained in detail in Table 1.

3 Estimation method

3.1 Failure criterion

Since it has been proven that the failure mode of load-bearing wall is out-of-plane bending failure, similar to the static load condition (Zhang, 2005), cracks and inclination should be important indicators of the failure criterion of load-bearing wall attacked by debris flow. Additionally, several damage classifications of brick and concrete building from occupational criterions are also taken into considered (Qian, 2013). Then, the failure criterion for the load-bearing wall of brick concrete building attacked by debris flow vertically is established in Table 2. However, directly applying this criterion will lead the unreasonable result when the value near the critical number is being judged. In this case, Fuzzy mathematical theory is helpful to solve this problem.

3.2 Estimation method based on Fuzzy mathematics

Based on Fuzzy mathematics, the procedure of estimation method for the wall damage degree (vulnerability) is stated as following.

NHESSD
3, 5015–5044, 2015

1. Single index evaluation

$U = \{a,\ b,\ c,\ d\}$ is the influence indicators aggregate and a, b, c, d denote the influence indicators listed in Table 2 respectively. $T = \{\mathrm{I},\ \mathrm{II},\ \mathrm{III},\ \mathrm{IV}\}$ is the damage results aggregate. Then, the fuzzy relation between influence indicators and damage results can be represented with evaluation matrix **R**.

$$\mathbf{R} = \begin{bmatrix} r_{11} & r_{12} & r_{13} & r_{14} \\ r_{21} & r_{22} & r_{23} & r_{24} \\ r_{31} & r_{32} & r_{33} & r_{34} \\ r_{41} & r_{42} & r_{43} & r_{44} \end{bmatrix} \tag{1}$$

In which $r_{mn} = \mu_{T_n}(U_m)$ $(0 \le r_{mn} \le 1,\ 1 \le m \le 4,\ 1 \le n \le 4)$ denotes the membership degree of the result element T_n from the view of the indicator element U_m; $\mathbf{R}_m = (r_{m1}, r_{m2}, r_{m3}, r_{m4})$ is the assessment aggregate of U_m and also the fuzzy subset of T. The membership function $\mu_{T_n}(U_m)$ has the formulas below respectively.

$$\mu_{\mathrm{I}}(U_m) = \begin{cases} 1, & U_m \le k_{m1}; \\ (k_{m2} - U_m)/(k_{m2} - k_{m1}), & k_{m1} < U_m \le k_{m2}; \\ 0, & \text{otherwise} \end{cases} \tag{2}$$

$$\mu_{\mathrm{II}}(U_m) = \begin{cases} (U_m - k_{m1})/(k_{m2} - k_{m1}), & k_{m1} < U_m \le k_{m2}; \\ (k_{m3} - U_m)/(k_{m3} - k_{m2}), & k_{m2} < U_m \le k_{m3}; \\ 0, & \text{otherwise} \end{cases} \tag{3}$$

$$\mu_{\mathrm{III}}(U_m) = \begin{cases} (U_m - k_{m2})/(k_{m3} - k_{m2}), & k_{m2} < U_m \le k_{m3}; \\ (k_{m3} - U_m)/(k_{m3} - k_{m2}), & k_{m3} < U_m \le k_{m4}; \\ 0, & \text{otherwise} \end{cases} \tag{4}$$

NHESSD
3, 5015–5044, 2015
The quantitative estimation of the vulnerability of brick
J. Zhang et al.

$$\mu_{\rm IV}(U_m) = \begin{cases} (U_m - k_{m3})/(k_{m4} - k_{m3}), & k_{m3} < U_m \le k_{m4}\ ; \\ 1, & U_m > k_{m4}\ ; \\ 0, & \text{otherwise} \end{cases} \tag{5}$$

In which the matrix $K_m = (k_{m1}, k_{m2}, k_{m3}, k_{m4})$ denotes the membership matrix of a influence indicator; $k_{m1} \sim k_{m4}$ are the evaluation parameters of the four indicators in Table 2. The parameter adopts the mean value of the adjacent critical number. For example, the matrix of the maximum crack width $K_1 =$ (0.1, 0.3, 0.55, 0.8). Thus, the evaluation matrix **R** can be obtained by the Eqs. (2)–(5).

2. Weight determination

The weight determination mostly considers the over-limit of indicator. With the normalization the weight of indicators are obtained by Eq. (6). The weights of the four indicators compose the weight matrix $\mathbf{A} = [W_a, W_b, W_c, W_d]$.

$$W_{U_m} = \frac{P_{U_m}/S_{U_m}}{\sum\limits_{m=1}^{4} (P_{U_m}/S_{U_m})} \tag{6}$$

In which P_{U_m} is the measured value of influence indicator; S_{U_m} is the mean value of all critical numbers. For example, the critical numbers of the maximum crack width are 0.2, 0.4 and 0.7 mm, then $S_a = (0.2 + 0.4 + 0.7)/3 = 0.433$ mm.

3. Vulnerability assessment

Multiply the matrix **A** and evaluation **R**, then generating a new matrix $[x_1, x_2, x_3, x_4]$, in which $x_1 + x_2 + x_3 + x_4 = 1$. x_1, x_2, x_3, x_4 represent the membership degree of indicators to the damage levels (I, II, III and IV) respectively. The loss percentage l_n for all the damage levels are:

a. slight damage: 0–10 %, I_1 = 10 %;

b. minor damage: 10–30 %, I_2 = 30 %;

c. mediate damage: 30–60 %, I_3 = 60 %;

d. serious damage or collapse: 60–100 %, I_4 = 100 %.

As shown above, adopting the upper limit of loss lead the conservation result which will overestimate the loss. Finally the vulnerability assessment is determined as following:

$$V = \sum_{n=1}^{4} (I_n \cdot x_n). \tag{7}$$

4 Results and analysis

4.1 Damage description

Three type of load are discussed as follows to be the candidate of the disaster-causing factor (debris flow) in vulnerability curve:

1. Momentum: the velocity and flow depth are the basic physical descriptor of debris flow in unit width. Momentum includes both these two descriptors and can demonstrate the energy of debris flow.

2. Maximum impact force: according to momentum theorem $mv = Ft$, the impact force will increases with the decrease of time when the momentum stays the same. Actually, the large load which exceeds the material strength is the essential reason of structure failure. Therefore, maximum impact force should be taken into the consideration.

NHESSD
3, 5015–5044, 2015

3. Maximum impact bending moment: as mentioned above, the out-of-plane bending failure is the failure mode of brick and concrete wall. The impact bending moment also contains the velocity and flow depth. Therefore, it is reasonable to consider the maximum impact bending moment as the candidate of disaster-causing factor. In order to choose the best disaster-causing factor from the candidates, analysis and comparison are conducted through the experiments. The momentum, maximum impact force and maximum impact bending moment in each condition of the experiments are listed in Table 3.

Figures 3–5 show the cracks in series A, B and C experiments respectively. The crack distribution is analyzed from two aspects – under the same height of board and the same falling height.

4.1.1 The same height of board

Taking the 1.0 m depth for example, the crack distributions of series A are shown in Fig. 3 (different energy of the sphere or flow velocity). In A1, A2 and A3, the ratio of both maximum impact force and bending moment is 1 : 1.15 : 2.62 and the ratio of momentum is 1 : 1.76 : 2.4. Under the same flow depth, the crack width, length and quantity will increase when the load acting on the wall becomes larger. In A1 experiment, the wall keeps completeness except for several short and tiny cracks among which the maximum width is 0.2 mm and the maximum length is 273 mm. In A2 experiment, the cracks is wider spreading in horizontal direction. Part of the wall has dropped the surface layer due to the deformation and tremor. Most of the cracks are 0.1–0.2 mm width. The maximum width of crack is 0.4 mm and the maximum length is 2022 mm. In A3 experiment, the cracks spread out of the cover area of broad. Both the cracks in horizontal and vertical direction extend constantly to the edge of wall. Thus, the wall has seriously visible deformation in profile and more surfer layer has dropped from the wall. The maximum width of crack is 1 mm and the maximum length is 3216 mm. For

NHESSD
3, 5015–5044, 2015

the 1.5 and 2.0 m experiments, the conclusions of the cracks development with the impact load are similar.

4.1.2 The same falling height

Taking the iron sphere that is 86 kg weight falling from 3 m height for example (different height of the board or flow depth), the crack distribution of A2, B2 and C2 experiment is shown in Figs. 3b, 4b and 5b respectively. The measured impact force in these three experiments is 45, 23.2 and 28 kN respectively. It is found that the measured data of series B is lower than expected value. There are possibly at least three factors that can influence the force impacting on the wall: first, since the experiments were conducted in outdoor lab, the weather, for example wind can accelerate or decelerate the velocity of the iron sphere depending on their relative movement direction; Second, the friction of the shaft which should be conquered by sphere will also reduce the actual velocity of sphere; three, when the dynamic system is off, the residual sticking force between the sphere and the switch will decrease the energy of sphere. From the comparison of three figures, the total area and maximum length of crack in C2 experiment exceed those in A2 experiment even though the impact force in A2 is 1.6 times larger than that in C2. Table 4 includes the measured data of vulnerability indicators and the final vulnerability evaluation based on the proposed method. The vulnerability in C2 is 1.5 times larger than that in A2 and the dynamic displacement in A2 and C2 is 3.8 and 5.5 mm respectively. Therefore it might be deduced that the cracks mainly caused by the dynamic displacement when the wall is swinging under the impact force.

4.2 Vulnerability curve

Based on the failure criterion in Table 2, the indicators of all the experiments are collected in Table 4 below.

Assuming a piecewise function to represent the vulnerability curves, the curve is consisted of three lines: (1) at the first level of vulnerability, the value is a constant 10 %.

(2) The vulnerability linearly varies with the disaster intense factor when the value is between 10–100 %. (3) The vulnerability keeps 100 % even if the loads increase. Then draw the experimental data with momentum, maximum impact force and maximum bending moment in Figs. 6–8 respectively.

4.2.1 Momentum

From Fig. 6, it can be found that the vulnerability have a linear relation with the momentum and the data of same momentum (different height of board or flow depth) is clustering together. However, the momentum here is just theoretical value and there exist some energy loss when the sphere attacks the wall. The inelastic collision of the sphere and the board will reduce the energy. The rubber cushion between the board and the wall will also absorb part of the energy. Therefore, the actual momentum on the wall is less than the theoretical one. Unfortunately, no function can be applied to accomplish the transformation between them. As a result, the momentum in Fig. 6 is not reliable to establish the function with vulnerability.

4.2.2 Maximum impact force

According to the assumption of the vulnerability function, the piecewise function with maximum impact force is written as Eq. (8) and the fitting curve is drawn in Fig. 7. The relation coefficient r is 0.78. From Fig. 7, it can be observed that the data are not closely clustering around the curve.

$$\begin{cases} V = 0.1 & F \leq 11.87\,\text{kN} \\ V = 0.014F - 0.063 & 11.87\,\text{kN} < F \leq 77.34\,\text{kN} \\ V = 1 & F > 77.34\,\text{kN} \end{cases} \tag{8}$$

NHESSD
3, 5015–5044, 2015

4.2.3 Maximum bending moment

The maximum bending moment is defined as the multiplication of the maximum impact force F and the arm of uniform force $L = h/2$. The piecewise function with maximum bending moment is written as Eq. (9) and the fitting curve is drawn in Fig. 8. The relation coefficient is 0.87 which is more than the coefficient with maximum impact force. From the comparison of these two figures, it can be observed that the curve with bending moment have the better fitting with the measured data. If the wall is not breakdown by the impact force, then the wall will swing producing the dynamic displacement due to the bending moment since the reinforced concrete foundation is immobile. Part of the deformation can recover while others cannot. The cracks and the static displacement are the unrecovered deformation and the cracks of wall are caused by the tension stress during the swing. As a result, the maximum bending moment is more reasonable to be the disaster intense factor of the vulnerability of the brick and concrete building.

$$\begin{cases} V = 0.1 & F \cdot L \leq 11.75\,\mathrm{kN} \cdot m \\ V = 0.024(F \cdot L) - 0.18 & 11.75\,\mathrm{kN} \cdot m < F \cdot L \leq 49.46\,\mathrm{kN} \cdot m \\ V = 1 & F \cdot L > 49.46\,\mathrm{kN} \cdot m \end{cases} \quad (9)$$

5 Discussion

According to momentum theorem, the length of the collision duration which depends on the characteristics of materials (such as elastic modulus and Poisson ratio) decides the value of the impact force when the momentum is the same. However, the characteristics of materials are different from each other leading rather different results during the collision. For example, the impact force between iron materials is two times larger than the rock materials (or concrete materials) due to the different elastic modulus. Theoretically, the collision between rock and concrete can better simulate the impact process of debris flow while the impact substitute will be voluminous and could be damaged after several experiments since the density and hardness of rock is not large enough. In the experiments, both the impact substitute and the board are made of iron of which the elastic modulus is huge. The direct collision therefore, will create huge force beyond the reasonable value range in debris flow. However, Rubber's elastic modulus is rather small so the elastic modulus of the composite medium consisted of rubber cushion and iron board is between the two single mediums. With the increasing thickness of the rubber cushion, the elastic modulus of the composite medium will decrease.

Generally, the elastic modulus of the composite medium should be adjusted to the measured data in history events through preliminary experiments. Unfortunately, rare data of the impact force was recorded in prototype since debris flow always occurred abruptly. In the experiments, the wall cracks had approximate uniform distribution and the damage degree was expressed from slight to serious under the different loads. It is can be concluded that the design of experiments is reasonable to present the structure (brick and concrete) damage induced by debris flow. Because of the manufacture technology limit, the iron board, the rubber cushion and the wall cannot uniformly stick with each other exactly leading the deviation to ideal load which should be absolutely uniform.

6 Conclusion

The results of experiments demonstrate that the maximum impact bending moment is the principal reason of the wall damage and is more suitable to be the disaster-causing factor in the vulnerability curve of debris flow compared with the maximum impact force. The results verify the conclusion of Zhang's (2005) research further and in turn it also proves the reliability of the experiment results. Since it takes long time to curing the concrete and cost much to build the models, the experimental data is limit but precious for vulnerability research of debris flow. The curve and formula proposed above need field observation and more researches in further to be more reliable. Vulnerability study is much concern on the type of the vulnerable element. The curve and formula need

NHESSD
3, 5015–5044, 2015

modification when they are applied on the similar element constructed with brick and concrete.

Author contributions. J. Zhang, H. Qian and Z. X. Guo designed the experiments. H. Qian carried the experiments out and processed the data. J. Zhang prepared the manuscript with contributions from all co-authors.

Acknowledgement. The authors thank the support from the National Natural Science Foundation of China (No. 51409224) and the open fund program of SKLH, Sichuan University, China (No. 1312). The research also have been supported by the key laboratory of fluid and power machinery, ministry of education, Xihua University.

References

Bell, R. and Glade, T.: Quantitative risk analysis for landslides – Examples from Bíldudalur, NW-Iceland, Nat. Hazards Earth Syst. Sci., 4, 117–131, doi:10.5194/nhess-4-117-2004, 2004.

Chen, H., Tang, H. M., Xian, X. F., and Zhang, Y. P.: Experimental model of debris flow impact features, J. Chongqing Univ., 33, 114–119, 2010.

Cui, P.: Advances in debris flow prevention in China, Sci. Soil Water Conserv., 7, 7–13, 2009.

Douglas, J.: Physical vulnerability modelling in natural hazard risk assessment, Nat. Hazards Earth Syst. Sci., 7, 283–288, doi:10.5194/nhess-7-283-2007, 2007.

Earthquakes in China: available at: http://www.ceic.ac.cn/, last access: 12 June 2015.

Fuchs, S., Heiss, K., and Hübl, J.: Towards an empirical vulnerability function for use in debris flow risk assessment, Nat. Hazards Earth Syst. Sci., 7, 495–506, doi:10.5194/nhess-7-495-2007, 2007.

Haugen, E. D. and Kaynia, A. M. (Eds.): Vulnerability of Structures Impacted by Debris Flow, Taylor and Francis Group, London, 2008.

HAZUS: Multi-hazard Loss Estimation Methodology, Earthquake Model, HAZUS MH-MR2, User Manual, FEMA and NIBS, Washington, USA, 2006.

Hübl, J. and Fiebiger, G. (Eds.): Debris Flow Mitigation Measures, Springer-Verlag, New York, 2005.

Liu, K. F., Lee, H. C., and Wu, Y. H.: Assessment social impact of debris flow disaster by social vulnerability index, in: Kyoto Conference Proceeding, Kyoto, 24–31, 2012.

NHESSD

3, 5015–5044, 2015

Liu, X. L., Mo, D. W., and Wang, X. D.: Regional vulnerability assessment of debris flows, Chin. J. Geol. Hazard Cont., 12, 7–12, 2001.
Mavrouli, O. and Corominas, J.: Vunerability of simple reinforced concrete buildings to damage by rockfalls, Landslides, 7, 169–180, doi:10.1007/s10346-010-0200-5, 2010.
Michael, L., Baynes, F., Scott, G., and Granger, K.: Regional landslide risk to the cairns community, Nat. Hazards, 30, 233–249, 2003.
Papathoma, K. M., Kappes, M., Keiler, M., and Glade, T.: Physical vulnerability assessment for alpine hazards: state of the art and future needs, Nat. Hazards, 58, 645–680, doi:10.1007/s11069-010-9632-4, 2011.
Qian, H.: Study of vulnerability based on debris flows dynamic factors, Master Thesis, Sichuan Univ., Chengdu, 2013.
Quan Luna, B., Blahut, J., van Westen, C. J., Sterlacchini, S., van Asch, T. W. J., and Akbas, S. O.: The application of numerical debris flow modelling for the generation of physical vulnerability curves, Nat. Hazards Earth Syst. Sci., 11, 2047–2060, doi:10.5194/nhess-11-2047-2011, 2011.
Rickenmann, D.: Empirical relationships for debris flows, Nat. Hazards, 19, 47–77, 1999.
Romang, H. (Eds.): Wirksamkeit and Kosten von Wildbach-Schutzmassnahmen, Verlag des Geographischen Instituts der Universität Bern, Bern, Switzerland, 2004.
Tang, C., Zhang, J., and Zhou, C. H.: Vulnerability assessment of urban debris flow hazard, J. Catastrophol., 20, 11–17, 2005.
Tang, C., Rengers, N., van Asch, Th. W. J., Yang, Y. H., and Wang, G. F.: Triggering conditions and depositional characteristics of a disastrous debris flow event in Zhouqu city, Gansu Province, northwestern China, Nat. Hazards Earth Syst. Sci., 11, 2903–2912, doi:10.5194/nhess-11-2903-2011, 2011a.
Tang, C., Zhu, J., Ding, J., Cui, X. F., Chen, L., and Zhang, J. S.: Catastrophic debris flows triggered by a 14 August 2010 rainfall at the epicenter of the Wenchuan earthquake, Landslides, 8, 485–497, doi:10.1007/s10346-011-0269-5, 2011b.
Tie, Y. B.: The methodology and framework study of urban debris flow risk assessment, PhD thesis, Chengdu University of Technology, Chengdu, 2009.
Totsching, R., Sedlacek, W., and Fuchs, S.: A quantitative vulnerability function for fluvial sediment transport, Nat. Hazards, 58, 681–703, 2011.
Wang, Z. Y.: Experimental study on debris flow head and the energy theory, J. Hydraul. Eng., 3, 18–26, 2001.

NHESSD
3, 5015–5044, 2015

Zhang, J., Guo, Z. X., Cao, S. Y., and Singh, V. P.: Scale model for the confluent area of debris flow and main river: a case study of the Wenjia Gully, Nat. Hazards Earth Syst. Sci., 13, 3083–3093, doi:10.5194/nhess-13-3083-2013, 2013.

Zhang, Y.: Dynamic response of mountainous civil architecture in east China impacted by debris flows, PhD thesis, Institute of Mountain Hazards and Environment, CAS, Chengdu, 2005.

Table 1. Conditions of the experiments.

No.	A1	A2	A3	B1	B2	B3	C1	C2	C3
Height of board (m)	1	1	1	1.5	1.5	1.5	2	2	2
Height of falling (m)	3	3	5	3	3	5	3	3	5
Weight of sphere (kg)	49	86	86	49	86	86	49	86	86

NHESSD
3, 5015–5044, 2015

Table 2. Failure criterion for the load-bearing wall of brick concrete building attacked by debris flow.

Damage level	Maximum crack width/mm	Maximum crack length/mm	Total area of cracks mm^{-2}	Inclination/10^{-3}	Damage description	Required repair
I	0–0.2	0–750	0–500	0–1	slight	simple
II	0.2–0.4	750–1500	500–1000	1–1.5	minor	minor
III	0.4–0.7	1500–2250	1000–2000	1.5–2	mediate	mediate
IV	>0.7	2250–3000	2000–3500	2–2.5	serious	thorough repair or rebuild

NHESSD
3, 5015–5044, 2015

Table 3. Loads in experiments.

Type of load	A1	A2	A3	B1	B2	B3	C1	C2	C3
Momentum ($kg\,m\,s^{-1}$)	329	577.4	789.5	310.6	545.1	766.2	291	510.8	742.2
Maximum impact force (kN)	39	45	102.3	20.6	23.2	45.8	29.4	28	80.7
Maximum impact bending moment (kN m)	18	22.5	51.15	15.45	17.4	34.35	29.4	37.5	80.7

NHESSD
3, 5015–5044, 2015

The quantitative estimation of the vulnerability of brick

J. Zhang et al.

Table 4. Statistical table of the influence indicators.

No.	Cracks Maximum width (mm)	Maximum length (mm)	Total area (mm^2)	Inclination (10^{-3})	Maximum dynamic displacement (mm)	Vulnerability	Crack description
A1	0.2	273	45.1	0.89	2.4	18.4 %	A few and tiny
A2	0.4	2022	611.2	1.41	3.8	48.2 %	More and wider
A3	1	3267	2944.3	5.00	13.5	100.0 %	Constantly extend to the edge; Spread out of the board
B1	0.1	204	48.9	0.78	2.1	14.0 %	A few and tiny
B2	0.3	984	961.2	1.22	3.3	31.4 %	More and wider
B3	0.7	3216	4196	1.00	2.7	90.6 %	Constantly extend to the edge; Spread out of the board
C1	0.1	591	303.1	1.22	3.3	21.0 %	Separated and tiny
C2	0.3	2475	1296	2.04	5.5	70.9 %	More and wider
C3	1.1	3208	4192.7	1.96	5.3	96.8 %	Constantly extend to the edge; Spread out of the board

NHESSD
3, 5015–5044, 2015

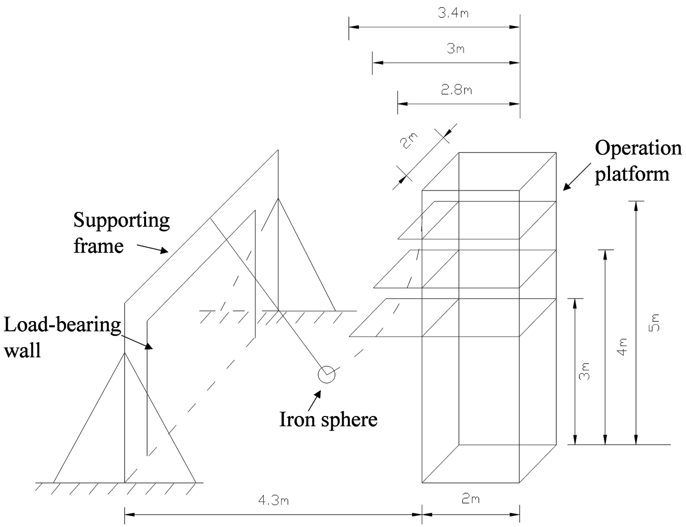

Figure 1. Experiment set up.

NHESSD
3, 5015–5044, 2015

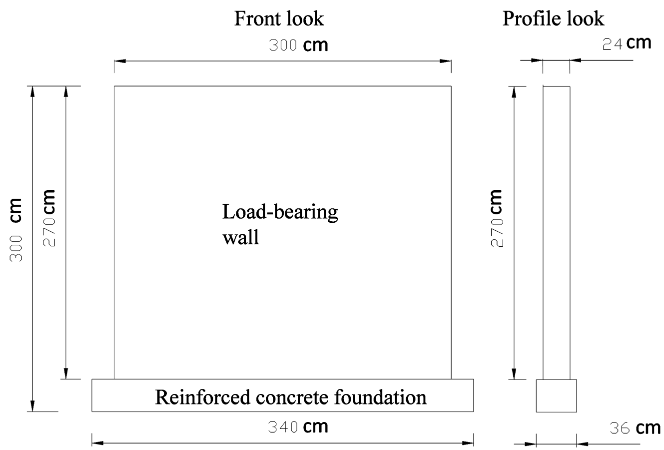

Figure 2. Sketch of standard load-bearing wall.

NHESSD
3, 5015–5044, 2015

The quantitative estimation of the vulnerability of brick

J. Zhang et al.

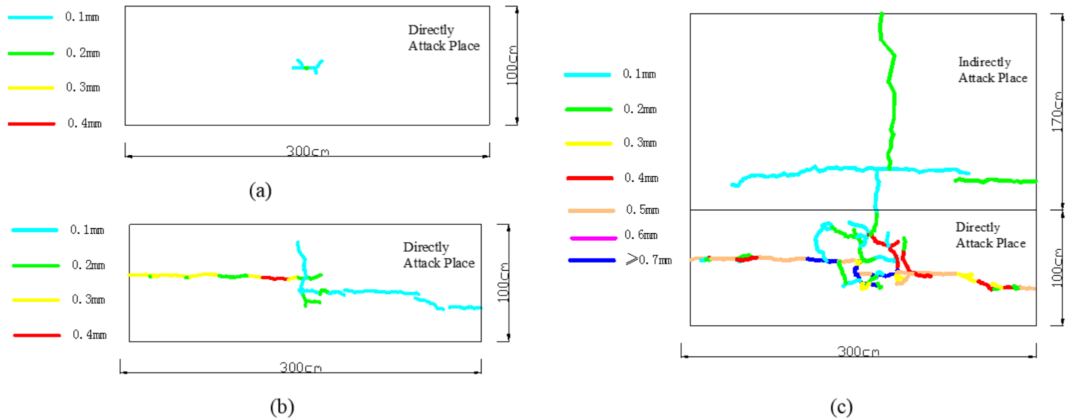

Figure 3. Distribution of the cracks on the element in series A (**a**, **b**, **c** represent the A1, A2 and A3 repectively).

NHESSD
3, 5015–5044, 2015

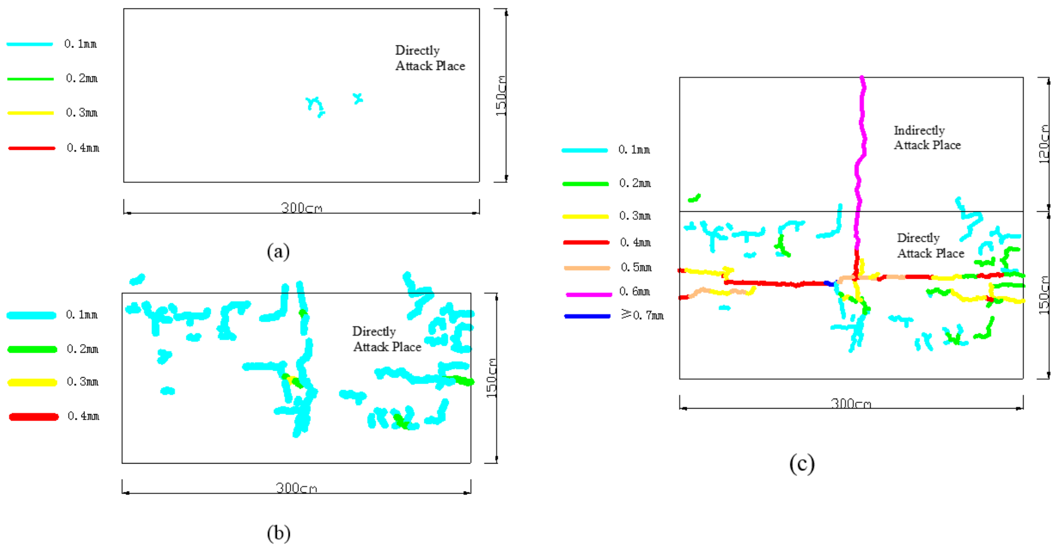

Figure 4. Distribution of the cracks on the element in series B (**a**, **b**, **c** represent the B1, B2 and B3 repectively).

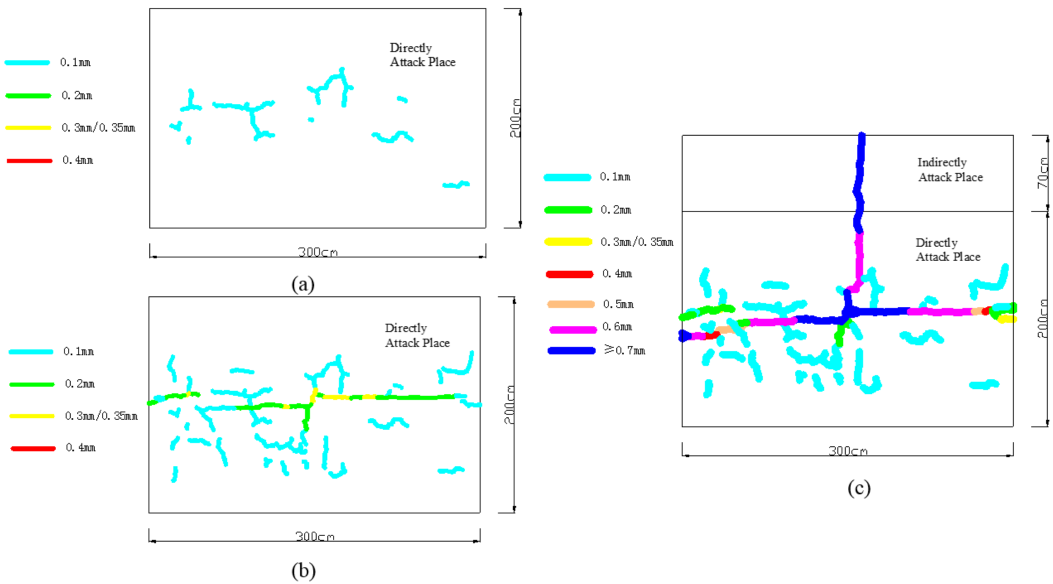

Figure 5. Distribution of the cracks on the element in series C (**a**, **b**, **c** represent the C1, C2 and C3 repectively).

NHESSD
3, 5015–5044, 2015

The quantitative estimation of the vulnerability of brick

J. Zhang et al.

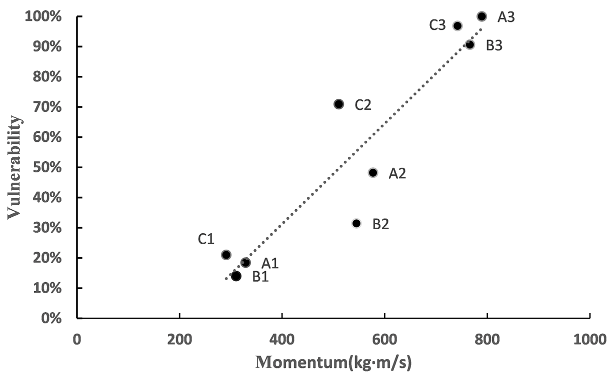

Figure 6. Vulnerability scatter chart with momentum.

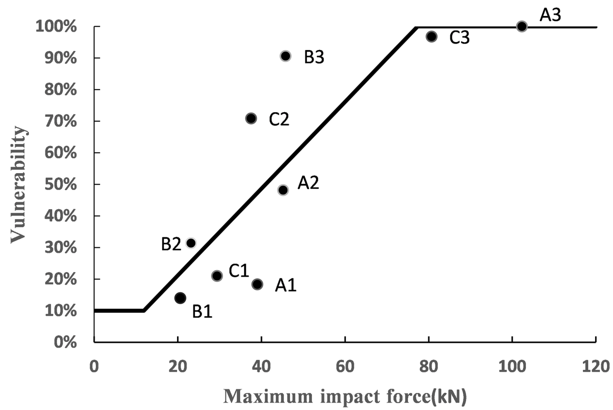

Figure 7. Vulnerability curve with maximum impact.

NHESSD
3, 5015–5044, 2015

The quantitative estimation of the vulnerability of brick

J. Zhang et al.

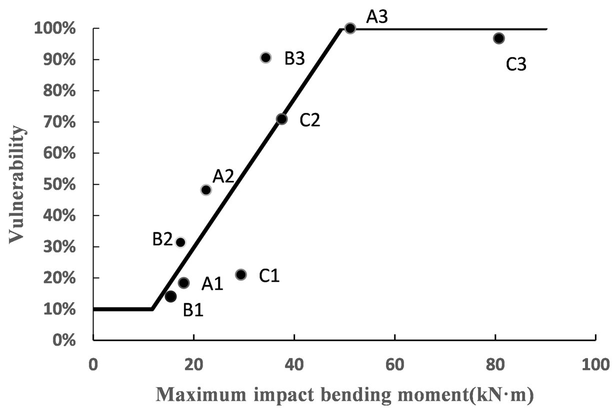

Figure 8. Vulnerability curve with maximum impact moment.

NHESSD
3, 5015–5044, 2015

The quantitative estimation of the vulnerability of brick

J. Zhang et al.